

INFLUENCE OF RESONANCE CHANGER PARAMETERS ON THE RADIATED SOUND POWER OF A SUBMARINE

Sascha Merz, Nicole Kessissoglou and Roger Kinns

School of Mechanical and Manufacturing Engineering, The University of New South Wales, Sydney NSW 2052, Australia

sascha.merz@gmx.net

Sound radiation from a submarine in the low frequency range is mainly due to fluctuating forces at the propeller. The forces arise due to the operation of the propeller in a non-uniform wake and are transmitted to the hull via the shaft and the fluid. The overall sound radiation from the submarine is the combination of sound radiated from the hull and sound radiated from the propeller. A hydraulic vibration attenuation device known as a resonance changer can be implemented in the propeller/shafting system in order to reduce the overall radiated sound power. In this paper, the influence of the virtual stiffness and damping of the resonance changer on the radiated sound power is investigated, where the importance of sound radiation from the propeller and the resulting re-excitation of the hull is of particular interest. Finite and boundary element methods are employed to model the structure and the fluid, respectively.

1. INTRODUCTION

The minimisation of sound radiated by a submarine is a significant research field as the importance of submarine stealth increases with more advanced detection techniques. A significant part of noise radiated from a submarine in the low frequency range can be correlated to the propeller. Broadband noise arises due to fluid flow over a wide frequency spectrum, however, tonal noise is prevalent in the low frequency range as shown in Fig. 1.

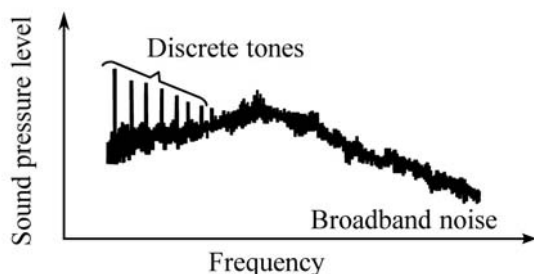


Figure 1. Non-cavitating noise of a submarine propeller [1]

The tonal noise can be correlated to the operation of the propeller in a non-uniform wake, as shown in Fig. 2. As the propeller blades pass through sections of different volume flow rate, they experience a temporal variation in drag. This results in a harmonically varying force on the propeller shaft as well as a harmonically varying pressure field originating from the propeller, at the blade-passing frequency (*bpf*) and its multiples [1, 2].

The pressure field as well as the structural force excite axial hull resonances correlated to accordion modes which are efficient sound radiators [4]. The first axial mode of a simplified submarine hull is depicted in Fig. 3. Furthermore, the structural force excites axial vibration of the propeller/shafting system, leading to additional sound radiation from the propeller. The overall radiated sound power is due to the combination of the sound fields radiated from the

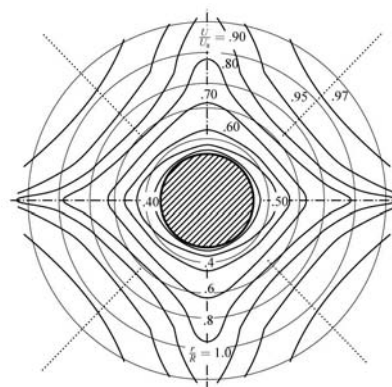


Figure 2. Wake of a torpedo [3]



Figure 3. First axial mode for a cylinder with rigid end plates and two internal bulkheads

propeller and the hull.

In order to minimise sound radiation correlated to propeller forces, a hydraulic vibration attenuation device known as a resonance changer (RC) can be implemented in the propeller/shafting system between the thrust bearing and the foundation, as shown in Fig. 4. It detunes the natural axial resonant frequency of the propeller/shafting system and dissipates vibratory energy by hydraulic means. This results in a reduction of axial propeller vibration as well as a reduction of the vibratory energy transmitted from the propeller to the hull. In addition, excessive vibration at hull or propeller/shafting system resonances may be avoided.

Dylejko used analytical models to find optimum parameters for the RC [5]. However, the complex interaction between the propeller and the hull via the fluid has been

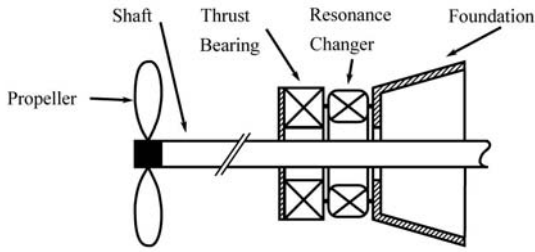


Figure 4. Propeller/shafting system

ignored as the use of analytical models requires numerous simplifications. For example, strong coupling between the structure and fluid cannot be considered for complex geometries. Numerical methods allow for more detailed models. A common approach is to use the finite element (FE) method to represent the structure and the boundary element (BE) method to represent the fluid [6, 7]. Strong coupling between non-matching meshes can be achieved by means of Lagrange multipliers at the fluid/structure interface in order to establish a coupled system [8].

In this work, a cost function is developed to assess the stealth of a submarine. For structural-acoustic optimisation, the integral of the overall radiated sound power over a predefined frequency range is often used [9, 10]. A simplified axisymmetric FE/BE model of a submarine is presented. The cost function is defined in terms of the overall radiated sound power due to sound radiation from the hull as well as sound radiation from the propeller. Scattering and re-excitation effects of the hull due to propeller noise are considered. The propeller is modelled as a rigid disc. The propeller/shafting system is represented by discrete finite elements, whereas the hull is modelled using shell elements based on Reissner-Mindlin theory. The fluid domain is represented using direct boundary elements. Results are presented for the cost function as a function of the stiffness and damping parameters for the RC.

2. PHYSICAL MODEL OF THE SUBMARINE

The simplified physical model of the submarine used in this paper is an extension of the model developed in [11]. In addition to the submarine hull, the propeller/shafting system and the tailcone have been included. The hull is considered as a thin-walled cylindrical shell with two evenly spaced internal bulkheads, rigid end plates at each end of the cylindrical hull and ring stiffeners. In addition, lumped masses are attached at the ends to represent the water in the ballast tanks and free flooded structures. The tail cone of the submarine is modelled as a rigid structure. The on-board machinery is considered as an added mass at the cylindrical shell surface. The model for the hull is depicted in Fig. 5.

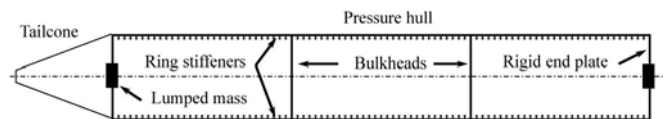


Figure 5. Submarine hull

A modular approach for the propeller/shafting system has been presented by Dylejko *et al.* [12]. The propeller/shafting system consists of the propeller, propeller shaft, thrust bearing, resonance changer and the foundation. The foundation is simplified to an axisymmetric, thin-walled, truncated cone attached to the stern side end plate of the pressure hull. Both the thrust bearing and resonance changer are represented by individual spring-mass-damper systems. The shaft and propeller can be envisaged as a solid rod with a lumped mass attached at the end. The effect of the entrained water at the propeller blades is taken into account as an additional lumped mass. The model for the propeller/shafting system is shown in Fig. 6, where f and v are the axial force and velocity components, respectively. m denotes a lumped mass. c and k are damping and stiffness coefficients, respectively. E and ρ denote Young's modulus and density, respectively. l_s is the propeller shaft length, l_{sc} is the effective propeller shaft length and A_s is the cross-sectional area of the propeller shaft. ν_f is the Poisson's ratio for the foundation, h_f is the foundation shell thickness, a is the foundation minor radius and b is the foundation major radius. 'p', 's', 'b', 'r', 'f' and 'h' denote parameters for the propeller, shaft, thrust bearing, resonance changer, foundation and hull, respectively.

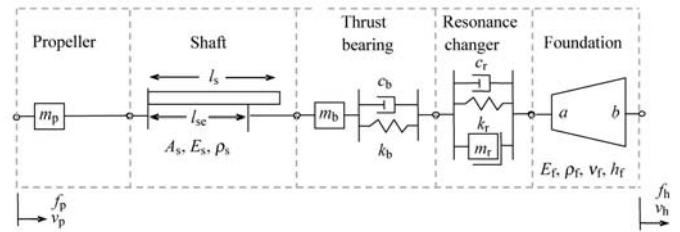


Figure 6. Modular approach for the propeller/shafting system [12]

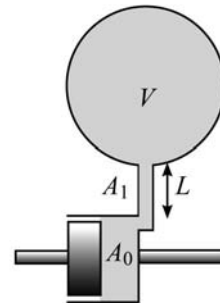


Figure 7. Resonance changer

The RC consists of a hydraulic cylinder that is connected to a reservoir by a pipe as shown in Fig. 7. The geometric properties of the assembly as well as the fluid properties determine the dynamic behaviour of the RC. It can be described as a spring-mass-damper system with the following virtual mass m_r , damping c_r and stiffness k_r parameters [13]:

$$m_r = \frac{\rho_r A_0^2 L}{A_1}; \quad c_r = 8\pi\mu L \frac{A_0^2}{A_1^2}; \quad k_r = \frac{A_0^2 B}{V}. \quad (1)$$

ρ_r is the density of the hydraulic medium, μ is the dynamic viscosity and B is the bulk modulus of the oil in the RC. V is

the volume of the reservoir, A_1 is the cross-sectional area of the pipe, L is the pipe length and A_0 is the cross-sectional area of the cylinder.

3. SOUND FIELD RADIATED BY THE PROPELLER

There are two mechanisms involved in the low frequency range that cause sound radiation from the propeller: (i) the operation of the propeller in a non-uniform wake and (ii) axial fluctuation of the propeller blades due to vibration of the propeller/shafting system. The overall sound radiation from the propeller can be simplified to a superposition of dipoles resulting from (i) and (ii), where a dipole is described as

$$p(r, \theta) = jkg(r)f \left(1 - \frac{j}{kr}\right) \cos \theta \quad (2)$$

where k is the wave number, θ is the angle between the field point direction and the force direction, f is the amplitude of the exciting force, r is the distance between the source and the field point and $g(r)$ is the free space Green's function. The directivity pattern of a dipole is shown in Fig. 8.

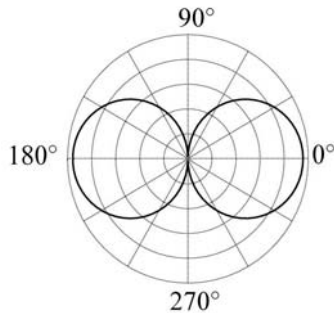


Figure 8. Dipole directivity pattern

A rigid disc approximation can be used to calculate the contribution from (ii). The force corresponding to the propeller axial velocity and the propeller added mass of water are expressed in terms of the radiation impedance as a function of wave number times disc radius [14].

4. NUMERICAL MODELLING

4.1 Sound Power Far Field Approximation

The radiated sound power through a surface Λ in the far field is given by [3]

$$\Pi \approx \frac{1}{2\rho c} \int_{\Lambda} pp^* d\Lambda \quad (3)$$

where p is the sound pressure, ρ is the density of the fluid and c is the speed of sound.

When Λ is subdivided into polygons and the pressure is expressed as a piecewise quadratic approximation, equation (3) can be represented in a discretised form similar to the procedure described in ref. [15]

$$\Pi = \mathbf{p}_{\Lambda}^H \Theta \mathbf{p}_{\Lambda}, \quad (4)$$

where \mathbf{p}_{Λ} is the vector of pressures in the integration points and the diagonal matrix Θ describes the geometry of Λ and the fluid properties.

4.2 Representation of the Acoustic Domain using BEM

The direct BEM is based on the Kirchhoff-Helmholtz integral equation [16]. An integral equation for a scattering problem can be obtained by using a combination of the Kirchhoff-Helmholtz integral equations for the interior and exterior problems [17]. Let Ω be the exterior acoustic domain and Γ is its boundary, then

$$c(P)p(P) = - \int_{\Gamma} \left(j\rho\omega v(Q)g(|P-Q|) + p(Q)\frac{\partial g(|P-Q|)}{\partial n} \right) d\Gamma(Q) + p_{inc}(P) \quad (5)$$

where P is the field point and Q is the source point, p is the pressure, v is the normal fluid particle velocity and p_{inc} denotes the pressure contribution from a discrete source such as a dipole. For a smooth boundary, $c(P) = \frac{1}{2}$ if $P \in \Omega$ and $c(P) = 1$ if $P \in \Gamma$.

For discretisation, the continuous integral equation is tested at a set of points P^* on Γ called collocation points, by employing $\delta(P - P^*)$ as a test function [7]. Subsequently Γ is subdivided into elements, where the field variables are elementwise interpolated through the collocation points. This allows for establishing a system of equations by numerical integration over the elements:

$$\mathbf{G}_{\Gamma} \mathbf{v}_{\Gamma} + \mathbf{H}_{\Gamma} \mathbf{p}_{\Gamma} = \mathbf{p}_{inc, \Gamma} \quad (6)$$

where \mathbf{v}_{Γ} and \mathbf{p}_{Γ} denote the normal fluid particle velocity and the surface pressure in the collocation points, respectively. The matrices \mathbf{G}_{Γ} and \mathbf{H}_{Γ} are called 'BEM influence' matrices. $\mathbf{p}_{inc, \Gamma}$ represents the pressure contribution from discrete sources in the collocation points of the surface Γ . For the presented models, $\mathbf{p}_{inc, \Gamma}$ has been evaluated using equation (2) to consider the dipole that is due directly to operation of the propeller in a non-uniform wake.

As the dipole pressure $\mathbf{p}_{inc, \Gamma, prop}$ due to axial propeller fluctuation depends on the axial surface normal velocity of the propeller, it can be expressed in terms of \mathbf{v}_{Γ} :

$$\mathbf{p}_{inc, \Gamma, prop} = \mathbf{G}_{\Gamma, prop} \mathbf{v}_{\Gamma} \quad (7)$$

The sparse matrix $\mathbf{G}_{\Gamma, prop}$ is computed using equation (2) together with the radiation impedance of the propeller [14] and subtracted from matrix \mathbf{G}_{Γ} to consider the additional dipole in the coupled system of equations.

The vector \mathbf{p}_{Λ} can also be obtained using the Kirchhoff-Helmholtz integral equation by numerical integration, once the pressure and normal velocity on the surface Γ are known:

$$\mathbf{p}_{\Lambda} = \mathbf{G}_{\Gamma\Lambda} \mathbf{v}_{\Gamma} + \mathbf{H}_{\Gamma\Lambda} \mathbf{p}_{\Gamma} + \mathbf{p}_{inc, \Lambda} \quad (8)$$

where $\mathbf{p}_{inc, \Lambda}$ is the pressure at the integration points of the surface Λ due to discrete sound sources. For the presented models, $\mathbf{p}_{inc, \Gamma}$ has been evaluated using equation (2) to consider the dipole that is due directly to operation of the propeller in a non-uniform wake. The contributions from the dipole that is due to axial propeller fluctuations has been considered by subtracting $\mathbf{G}_{\Lambda, prop}$ from $\mathbf{G}_{\Gamma\Lambda}$, where $\mathbf{G}_{\Lambda, prop}$ is obtained according to $\mathbf{G}_{\Gamma, prop}$ but for the surface Λ .

4.3 Representation of the Structural Domain using FEM

The structure that interacts with the fluid as well as the foundation of the propeller/shafting system is represented by a thin-walled axisymmetric shell of finite elements based on Reissner-Mindlin theory, where transverse shear stiffness is finite [18]. The stress component normal to the shell is assumed to be zero throughout the shell thickness. A simple, one-dimensional rod element has been used to model the section of the propeller shaft between propeller and thrust bearing. Lumped masses in the nodes were utilised to represent the propeller, the mass of the remaining section of the propeller shaft, the RC virtual mass, the mass of the thrust bearing and the lumped masses at the end plates. One-dimensional spring-damper elements were employed to represent the virtual stiffness and damping of the RC as well as the stiffness and damping of the thrust bearing. A detailed description of the aforementioned element types can be found in [19].

Applying the principle of D'Alembert, a finite element formulation for the structural part of the dynamic problem can be obtained. The finite element formulation can be expressed in matrix form

$$\mathbf{A}\mathbf{u} + \mathbf{L}_{sf}\mathbf{p}_\Gamma = \mathbf{f}_s, \quad (9)$$

where \mathbf{A} incorporates the structural stiffness, damping and mass matrices and \mathbf{L}_{sf} is a geometrical coupling matrix. The vector \mathbf{u} represents the nodal displacement for the FE mesh and \mathbf{f}_s is the load vector of concentrated forces.

4.4 Combined FE/BE Problem

Strong coupling of the acoustic BE and the structural FE models is achieved by imposing the following conditions at the structure/fluid interface; (i) the normal velocity of the structure equals the normal velocity of the fluid and (ii) the normal distributed surface load of the structure equals the acoustic surface pressure. Condition (ii) has already been implicitly considered in equation (9). For non-conforming meshes at the coupling interface, condition (i) cannot be considered in a strong sense. Therefore, an approach similar to that used in ref. [8] is employed, where the pressure can be interpreted as a Lagrange multiplier and continuity of the surface normal velocity is only established in a weak sense [20]. The resulting system of equations can be written as

$$\begin{bmatrix} \mathbf{A} & \mathbf{L}_{sf} \\ \mathbf{G}_\Gamma \mathbf{L}_{fs} & \mathbf{H}_\Gamma \end{bmatrix} \begin{Bmatrix} \mathbf{u} \\ \mathbf{p}_\Gamma \end{Bmatrix} = \begin{Bmatrix} \mathbf{f}_s \\ \mathbf{p}_{inc,\Gamma} \end{Bmatrix} \quad (10)$$

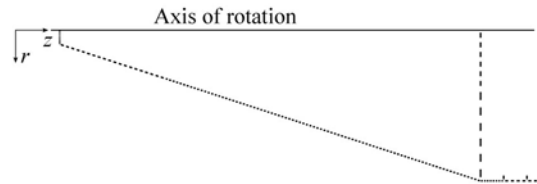
where \mathbf{L}_{fs} and \mathbf{L}_{sf} are geometrical coupling matrices.

When the solution vector of equation (10) is known, the pressure vector \mathbf{p}_Λ can be found using equation (8) and the identity $\mathbf{v}_\Gamma = \mathbf{L}_{fs}\mathbf{u}$, resulting in

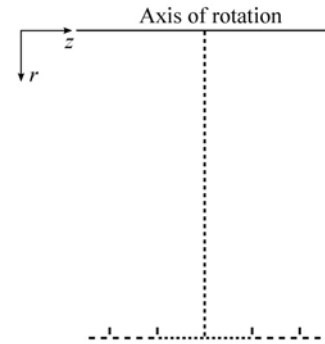
$$\mathbf{p}_\Lambda = [\mathbf{G}_{\Gamma\Lambda} \mathbf{L}_{fs} \quad \mathbf{H}_{\Gamma\Lambda}] \begin{Bmatrix} \mathbf{u} \\ \mathbf{p}_\Gamma \end{Bmatrix} + \mathbf{p}_{inc,\Lambda} \quad (11)$$

The radiated sound power can then be obtained using equation (4). A cost function representing the sound power over a given frequency range, can be defined as [9]

$$J = \frac{1}{\Delta\omega} \int_{\omega} \Pi d\omega. \quad (12)$$



(a) FE mesh at cone



(b) FE mesh at bulkhead

Figure 9. Details for the FE mesh of the submarine hull

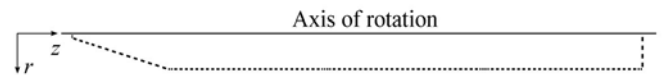


Figure 10. BE mesh of the submarine hull

5. RESULTS

Computations have been conducted for a fully coupled submarine model. ANSYS 11 was used to generate the FE and BE meshes and to compute the FE stiffness, mass and damping matrices. Details of the FE mesh for the submarine hull are shown in Fig. 9. The BE mesh is shown in Fig. 10

For both the FE and BE meshes, at least 10 elements per wave length were used. Computation of the BE and coupling matrices as well as equation solving was conducted by a software developed by the first author using SciPy and C++. Parameters for the propeller/shafting system and hull are given in Tables 1 and 2, respectively, as well as in ref. [14]. Results for the structural and acoustic responses are presented, where a fixed configuration of the RC parameters has been used (section 5.1) and for the cost function as defined in equation (12) (section 5.2). The fixed RC parameters were found by Dylejko *et al.* [12], where a simplified representation of the submarine hull was used and acoustic excitation was ignored. The results for the cost function were obtained by employing a frequency weighted, exciting force in order to take into account that the magnitude of the force is proportional to the square of the propeller rotational frequency. The force amplitude is defined as $(\omega/\Delta\omega)^2$, where a frequency range from 1 to 100 Hz was considered.

5.1 Structural and Acoustic Responses for fixed RC Parameters

The structural and acoustic responses of the submarine hull are presented, where the tailcone was modelled as a rigid structure. Both structural excitation through the

Table 1. Parameters for the propeller/shafting system

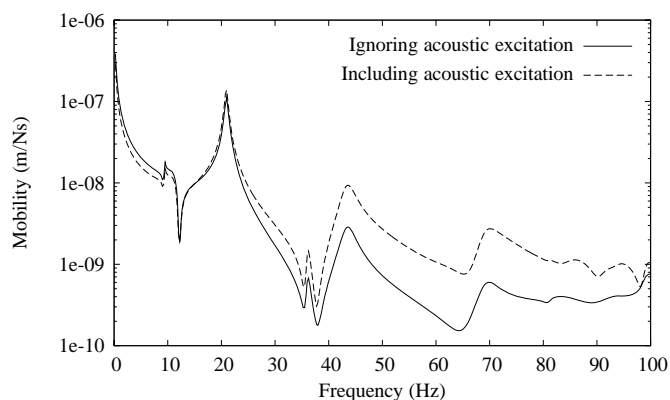
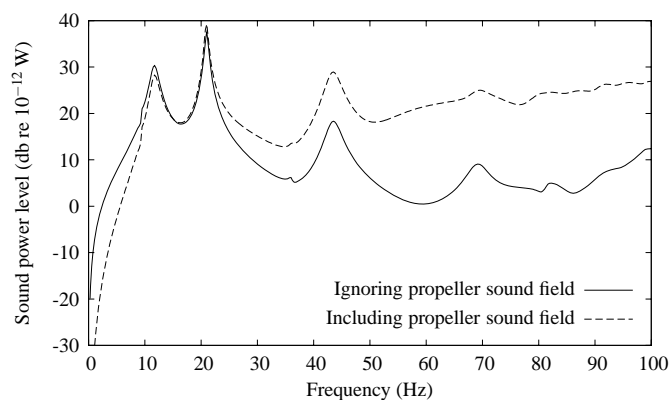
| Parameter | Value | Unit |
|-------------------------------|-------|----------------|
| Propeller diameter | 3.25 | m |
| Propeller structural mass | 10000 | kg |
| Propeller added mass of water | 11443 | kg |
| Shaft cross-sect. area | 0.071 | m ² |
| Shaft length | 10.5 | m |
| Effective shaft length | 9 | m |
| Resonance changer mass | 1000 | kg |

Table 2. Parameters for the hull

| Parameter | Value | Unit |
|--------------------------------|-------------------|----------------|
| Cylinder length | 45.0 | m |
| Cylinder radius | 3.25 | m |
| Shell thickness | 0.04 | m |
| Stiffener cross-sectional area | 0.012 | m ² |
| Stern lumped mass | 188×10^3 | kg |
| Bow lumped mass | 200×10^3 | kg |
| Cone length | 9.079 | m |

propeller/shafting system and acoustic excitation of the submarine hull have been considered. The acoustic excitation is due to dipole sound radiation caused by operation of the propeller in the non-uniform wake and axial propeller fluctuation due to vibration of the propeller/shafting system. The acoustic response in the far field is a combination of sound radiated from the submarine hull due to structural and acoustic excitation and sound radiated directly from the propeller. An exciting force of 1 N throughout the frequency range has been assumed.

Results for the structural response with and without the acoustic excitation are shown in Fig. 11. The three major peaks at about 20, 43 and 70 Hz represent the first three axial resonances of the hull. It can be seen that there occurs significant re-excitation of the hull due to the propeller sound field. The importance of the sound field radiated from the propeller becomes even more evident for the acoustic response of the submarine, as shown in Fig. 12. The radiated sound power is significantly increased at higher frequencies, when sound radiation from the propeller is taken into account. In addition, a peak can be identified at about 12 Hz that can

**Figure 11.** Mobility of the stern side end plate**Figure 12.** Sound power level for 1 N propeller force

be correlated to the fundamental resonant frequency of the propeller/shafting system.

5.2 Structural and Acoustic Responses for varying RC Parameters

By taking into account physical feasibility of the resonance changer, the RC virtual stiffness was varied between 15×10^6 and $1,500 \times 10^6$ N/m. A range from 5,000 to 1,100,000 kg/s was chosen for the RC virtual damping. A frequency range between 1 and 100 Hz was considered in order to cover sound radiation that is due to the first four harmonics of blade-passing frequency.

Results for the cost function are shown in Fig. 13. It can be concluded that an increase of the RC virtual damping generally leads to lower values for the cost function J . Two distinct local maxima of the cost function can be identified. The first local maximum occurs at the lower limits $c_r = 5,000$ kg/s and $k_r = 15 \times 10^6$ N/m for both the RC virtual damping and stiffness. In this case, the cost function is dominated by the sound power due to propeller vibration in the high frequency range, as shown in Fig. 14. This is due to the fact that a decrease of the values for c_r and k_r involves an increase of the propeller/shafting system axial flexibility. The second local maximum occurs at the upper limit $k_r = 1,500 \times 10^6$ N/m for the virtual stiffness and the lower limit $c_r = 5,000$ kg/s for the virtual damping. The cost function is dominated by sound radiation at the fundamental propeller/shafting system resonance. The global minimum occurs at the lower limit $c_r = 1,100,000$ kg/s for the virtual damping and $k_r = 540 \times 10^6$ N/m for the virtual stiffness. For the minimum cost function value, the radiated sound power at the fundamental hull resonance is negligible. Furthermore, the sound power due to propeller fluctuation in the high frequency range is low compared to the sound power for the RC configuration correlated to the first maximum.

6. CONCLUSIONS

A fully coupled vibro-acoustic model for a submarine has been developed in order to find optimum design parameters for a passive vibration attenuation device known as a resonance changer. The objective is to minimise the overall radiated sound power due to propeller forces in the low frequency range. The overall radiated sound power is due to

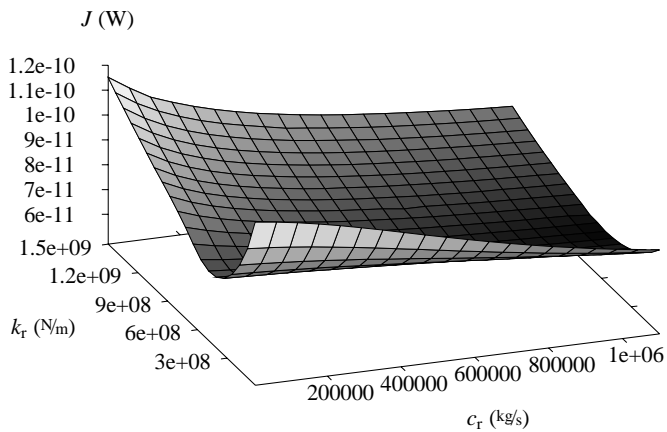


Figure 13. Cost function

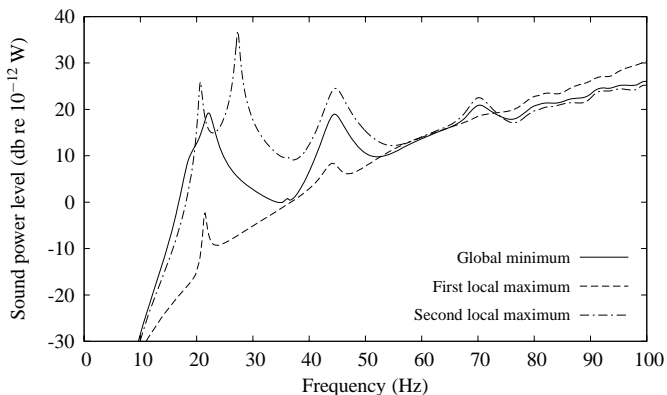


Figure 14. Sound power level for the minimum and maximum cost function values

sound radiated from the hull as well as sound radiated from the propeller, where the importance of sound radiation from the propeller was of particular interest. A cost function has been obtained by integration of the radiated sound power over the investigated frequency range.

The structural and acoustic responses of a fully coupled submarine model for fixed and varying RC parameters have been presented. In both cases, there is a significant influence on overall sound radiation and re-excitation of the structure due to the propeller sound field. The variation of the RC stiffness was shown to have a significant effect on the fundamental resonant frequency of the propeller/shafting system. In contrast, an increase of the RC damping leads to a reduction of sound radiation due to axial propeller vibration.

REFERENCES

[1] J. S. Carlton, *Marine Propellers and Propulsion*, Butterworth-Heinemann, Oxford, 1994.
 [2] O. Rath Spivack, R. Kinns and N. Peake, Acoustic excitation of hull surfaces by propeller sources. *Journal of Marine Science Technology* **9**, 109–116 (2004).
 [3] D. Ross, *Mechanics of Underwater Noise*, Peninsula Publishing, Los Altos, 1987.
 [4] C. Norwood, The free vibration behaviour of ring stiffened cylinders, Technical Report 200, DSTO Aeronautical and Maritime Research Laboratory,

Melbourne, Australia, 1995.

[5] P. G. Dylejko, *Optimum Resonance Changer for Submerged Vessel Signature Reduction*, PhD Thesis, School of Mechanical and Manufacturing Engineering, The University of New South Wales, Sydney, 2008.
 [6] S. Amini, P. J. Harris and D. T. Wilton, *Coupled Boundary and Finite Element Methods for the Solution of the Dynamic Fluid-Structure Interaction Problem*, Springer-Verlag, 1992.
 [7] S. Marburg and B. Nolte, editors, *Computational Acoustics of Noise Propagation in Fluids*, Springer-Verlag, Berlin, 2008.
 [8] F. B. Belgacem, The Mortar finite element method with Lagrange multipliers. *Numerische Mathematik* **84**(2), 173–197 (1999).
 [9] S. Marburg, Developments in Structural-Acoustic Optimization for Passive Noise Control. *Archives of Computational Methods in Engineering* **9**(4), 291–370 (2002).
 [10] J. S. Lamancusa, Numerical optimization techniques for structural-acoustic design of rectangular panels. *Computers & Structures* **48**(4), 661–675 (1993).
 [11] S. Merz, S. Oberst, P. G. Dylejko, N. J. Kessissoglou, Y. K. Tso and S. Marburg, Development of coupled FE/BE models to investigate the structural and acoustic responses of a submerged vessel. *Journal of Computational Acoustics* **15**(1), 23–47 (2007).
 [12] P. G. Dylejko, N. J. Kessissoglou, Y. K. Tso and C. J. Norwood, Optimisation of a resonance changer to minimise the vibration transmission in marine vessels. *Journal of Sound and Vibration* **300**, 101–116 (2007).
 [13] A. J. H. Goodwin, The design of a resonance changer to overcome excessive axial vibration of propeller shafting. *Institute of Marine Engineers—Transactions* **72**, 37–63 (1960).
 [14] S. Merz, R. Kinns and N. J. Kessissoglou, Structural and acoustic responses of a submarine hull due to propeller forces. *Journal of Sound and Vibration*, available online (2009).
 [15] R. R. Salagame, A. D. Belegundu and G. H. Koopman, Analytical sensitivity of Acoustic power radiated from plates. *Journal of Vibration and Acoustics-Transactions of the ASME* **117**(1), 43–48 (1995).
 [16] G. Kirchhoff, Zur Theorie der Lichtstrahlen. *Annalen der Physik* **254**(4), 663–695 (1883).
 [17] T. W. Wu, editor, *Boundary Element Acoustics*, WIT Press, Southampton, 2000.
 [18] O. C. Zienkiewicz and R. L. Taylor, *The Finite Element Method: Solid Mechanics*, Volume 2, Elsevier Butterworth-Heinemann, Amsterdam, London, 6th edition, 2005.
 [19] O. C. Zienkiewicz and R. L. Taylor, *The Finite Element Method: Its Basis and Fundamentals*, Volume 1, Elsevier Butterworth-Heinemann, Amsterdam, London, 6th edition, 2005.
 [20] D. Fritze, S. Marburg and H.-J. Hardtke, FEM-BEM-coupling and structural-acoustic sensitivity analysis for shell geometries. *Computers & Structures* **83**(2-3), 143–154 (2005).